

## CFD Assessment of Steady-State Heat Loss through Metal Containment of ATOM

Geonhyeong Lee<sup>1</sup>, Doyoung Shin<sup>1</sup>, Joongoo Jeon<sup>1</sup>, Taeseok Kim<sup>1</sup>, Yonghee Kim<sup>2</sup>, Sung Joong Kim<sup>1,3</sup>

<sup>1</sup>Department of Nuclear Engineering, Hanyang University  
222 Wangsimni-ro, Seongdong-gu, Seoul, 04763, Republic of Korea

<sup>2</sup>Department of Nuclear and Quantum Engineering, Korea Advanced Institute of Science and Technology, 291  
Daehak-ro, Yuseong-gu, Daejeon, 34141, Republic of Korea

<sup>3</sup>Institute of Nano Science & Technology, Hanyang University  
222 Wangsimni-ro, Seongdong-gu, Seoul, 04763, Republic of Korea  
ghlee9605@hanyang.ac.kr; dyshin@hanyang.ac.kr; jgjeon@hanyang.ac.kr; tkim@hanyang.ac.kr;  
yongheekim@kasit.ac.kr; sungjkim@hanyang.ac.kr

### 1. Introduction

According to the IAEA, small modular reactor (SMR) is defined as a modularized small reactor that produces electrical power up to 300 MWe [1]. Recently, the SMR has received a worldwide attention for its potential advantages of enhanced safety, compact and simple design, lower capital cost, and power flexibility by deploying multi-modules [2-4]. An Autonomous Mobile On-Demand Reactor Module (ATOM) with a capacity of 150 MWe has also been developed by the multi-university research team centered through the KAIST in Korea.

The ATOM bears numerous innovative features such as soluble boron-free coolant system, supercritical CO<sub>2</sub> power conversion cycle with air-cooling system, and fully passive safety system [5-7]. The ATOM includes a distinct component of a double vessel structure of a metal containment vessel (MCV) surrounding a reactor pressure vessel (RPV). The double vessel structure forms a gap space (hereafter called MCV space) between the two vessels, which works as a buffer space to retain unwanted loss of coolant and possible fission product during a hypothesized transient.

During the normal operation, the MCV space acts as an insulator to prevent heat loss to the environment. Thus, it is necessary to fill the space by the material having poor heat transfer capability. As a candidate, maintaining the space in vacuum was envisioned by the NuScale for effectively eliminating the conduction and convection heat transfer. However, because maintaining vacuum space inevitably raises additional maintenance issues of vacuum pumping cost and possible leak from the RPV to the gap space, filling the gap with a stagnant gas at atmospheric pressure without control equipment has been proposed as an alternative.

In order to replace the vacuum gap condition with a gas-type gap filler, a reasonable level of insulation performance should be secured considering the normal operating condition. As of this writing, however, no systematic research has been reported on the comparison of insulation performance with potential gap material.

Thus, in this study computational fluid dynamics (CFD) simulations were performed on the ATOM under normal operating conditions to confirm if the gas-type gap filler will perform sufficient thermal insulation

performance in comparison with the vacuum. For potential gap filler material, argon, air, carbon-dioxide, and xenon has been screened out.

### 2. Computational fluid dynamics modeling

#### 2.1 Simulation overview

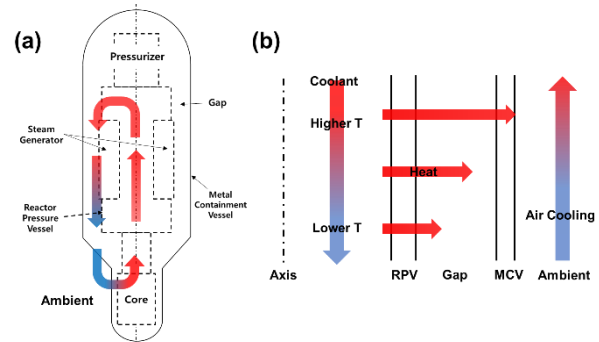


Fig 1. (a) A schematic and (b) heat loss mechanism of the ATOM

As shown in Fig. 1(a), the core at the bottom, the pressurizer at the top, and the steam generator at the center are located, and they are all integrated inside the RPV. The coolant circulates through the pump and transfers heat from the core to the steam generator, causing the secondary system to boil. During this process, a part of the heat of the primary system can be transferred through the gap and unnecessary heat loss occurs through the MCV outer surface.

Since each gas exhibits its own thermal-physical properties, the amount of heat loss is different for each gas. Among them, the optimal gas gap filler should have superior thermal insulation performance compared to other gases under normal operating conditions. Therefore, to compare the amount of heat loss, CFD simulation was performed by using ANSYS FLUENT 18.0 version. At this time, the vacuum conditions in Fluent were simulated by using thermo-physical properties of air at a pressure of 1 mbar by referring to NuScale and compared with gas-type gap fillers [8].

#### 2.2 Geometry and mesh

To evaluate the heat loss in ATOM, two-dimensional mesh was realized through the ANSYS Design Modeler 17.0. These values are summarized in Table I.

Table I. The size of the vessel components

Variable [m]	Size	Variable [m]	Size
MCV height	14.886	RPV height	13.440
MCV outer radius	2.022-2.273	RPV outer radius	0.84-1.68
MCV thickness	0.09	PRV thickness	0.13

In addition, to consider an infinite atmosphere surrounding the module, the sidewall was set at 6 m distant from the center so that it does not affect the module.

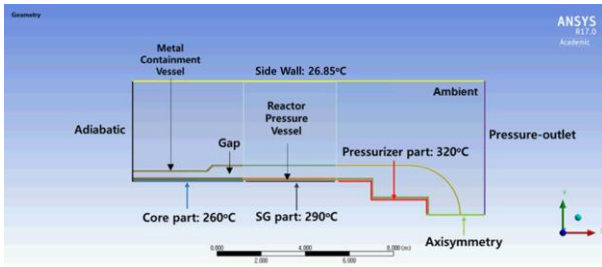


Fig 2. The boundary conditions

By appropriately setting boundary conditions for the formed two-dimensional mesh, a normal operation condition with a constant heat generation was simulated.

As shown in Fig. 2, the axisymmetric condition was applied by setting the x-axis as the centerline of symmetry. In addition, because the temperature of the RPV inner wall decreases by the temperature of the downflow coolant, it is divided into three parts to reflect this. The pressurizer, steam generator, and downcomer parts were set in order from the top to bottom, and respective regional temperatures were set to 320, 290, and 260 °C. The external wall temperature was set as default, 26.85 °C, the bottom was at adiabatic condition, and the top was set at a pressure-outlet condition so that outside air can flow in and out.

A mesh sensitivity analysis was conducted to verify the independence between meshes with different numbers of nodes by adjusting the cell size. Independence was confirmed among all meshes investigated, and in this study CFD calculation was performed by using a mesh with 2,135,664 nodes.

### 2.3 Solver setting

All simulations were performed in steady state and gravitational conditions. Particularly, in this study a radiation model was included as an option to assess the amount of heat loss due to the radiation heat transfer. The radiation model was used as the DO gray radiation model. The emissivity was set to 0.7 and 0.4 for the walls of the RPV and the MCV, respectively.

To simulate natural convection by buoyancy force, the density of each gas was set to be calculated by

Boussinesq approximation in Eq. (1). The values  $\beta$  and  $\rho_0$  were entered as the thermal expansion coefficients and densities at  $T_0$ .

$$\rho = \rho_0 - \beta\rho_0(T - T_0) \quad (1)$$

The solver settings were summarized in Table 2. In spatial discretization, the pressure term was modeled as body force weighted to simulate buoyancy. The gradient term was calculated based on the least squares cell and energy and momentum was calculated by the second order upwind. The rest was calculated by the first order upwind. Finally, the pressure-velocity coupling was used to perform an explicit interpretation of the steady-state, and the flow Courant number was set as 1 for the stable results.

Table II. Ansys fluent solver settings

<b>Viscous Model</b>		k-epsilon Realizable
<b>Density Model</b>		Boussinesq approximation
<b>Radiation Model</b>		DO gray Model
<b>Spatial Discretization</b>	<b>Gradient</b>	Least Squares Cell Based
	<b>Pressure</b>	Body Force Weighted
	<b>Momentum</b>	2 <sup>nd</sup> Order Upwind
	<b>Energy</b>	2 <sup>nd</sup> Order Upwind
<b>Pressure-Velocity Coupling</b>		Coupled
<b>Flow Courant Number</b>		1

### 3. Results and discussion

The ANSYS FLUENT allows to identify the heat loss mechanism and fluid behavior inside the gap and on the MCV wall during normal operation conditions. In this work, the convergence of computations was confirmed with the residuals of continuity, k and epsilon below  $1 \times 10^{-3}$ , and energy residual below  $1 \times 10^{-8}$ .

#### 3.1 Streamline of the flow in the gap

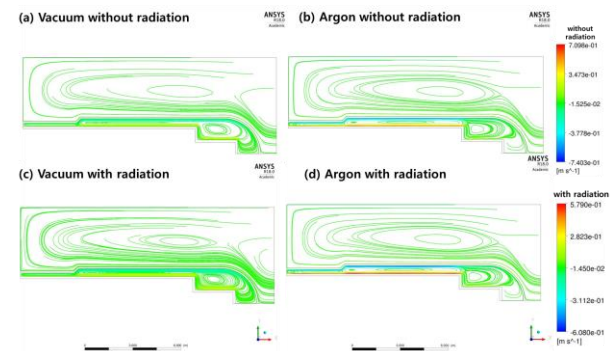


Fig 3. Streamline for vacuum (a, c) and argon (b, d)

In all gap fillers, natural convection was observed rising from the RPV outer wall and descending from the MCV inner wall. However, as the gap material changes, the thermal properties also change, so the internal flow also changes slightly.

Figure 3 shows the flow difference with or without radiation when the gap filler is vacuum and argon with streamlines. In the absence of radiation, it was confirmed that the flow due to natural convection inside the gap is relatively strong. This is because there is no heat transfer by radiation, so the heat escaping from inside the gap to the environment is relatively small. Therefore, as the energy of the inner fillers increases, the flow becomes faster.

In addition, it was confirmed that the flow of the gas-type filler was about 3 times faster than that of the vacuum condition. The density difference according to the temperature difference in the gap determines the strength of natural convection. In the vacuum conditions simulated in this calculation, the density change according to temperature is insignificant, but gas fillers exhibit relatively large changes. In addition, the very low density limits the transfer of intermolecular energy in a vacuum. For these reasons, the development of flow in vacuum conditions seems to be limited.

### 3.2 The total heat loss depending on the gap fillers

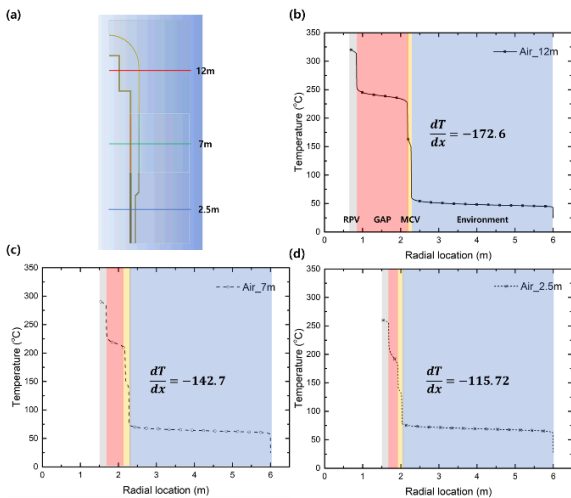


Fig 4. Temperature distribution of air depending on the height

Since there is a limit to accurately comparing the amount of heat loss by using the streamline only, the temperature distribution in the radial direction was estimated to calculate the temperature gradient in the MCV.

To calculate the heat loss to the outside, this value was applied to Fourier's law as in Eq. (2) to obtain the heat flux ( $q''$ ). At this time, in general when natural convection occurs, the upper side has a higher temperature, so the higher heat loss is measured. To reflect the heat loss that varies with height, each heat flux

was measured at heights of 2.5 m, 7 m, and 12 m. Figure 4 (a) shows the location where each temperature was measured.

$$\text{Fourier's law: } q'' = -k \frac{dT}{dx} \quad (2)$$

Figure 4 (b)-(d) shows the temperature distribution and temperature gradient at each height. Each region is identified by color and the temperature gradient in the MCV region shown in yellow is indicated in each graph. The temperature gradient at the higher position is larger, and the temperature gradient at the lower position is relatively small.

The total heat loss was then obtained by multiplying the area corresponding to the calculated heat flux. The calculated results are summarized in Table III.

Table III. The amount of total heat loss to environment

Material	w/o radiation	w/ radiation
Vacuum	5.04	330.43
Argon	99.22	374.71
Air	124.03	393.52
Carbon-dioxide	121.57	388.56
Xenon	74.96	360.36

In the absence of radiation, it was confirmed that vacuum has much better thermal insulation performance than other gases. This phenomenon occurs because the density of the vacuum condition is very low, and the distance between the molecules of the medium for conduction or convection is too far. For gases other than the vacuum, thermal insulation performance is determined according to thermal conductivity. Xenon, which has the lowest thermal conductivity, showed the highest insulation performance.

In the presence of radiative heat transfer, if heat loss by convection and conduction dominates, the total heat loss should still show a significant difference between vacuum and gases. However, the heat loss estimate did not show a significant difference between vacuum and gas fillers, indicating that radiation heat transfer was predominant.

The insulation performance is still the best under vacuum conditions, but the difference with gas fillers is reduced to a level of 10-20%. In particular, in case of xenon, it was confirmed that it is the optimal gas gap filler, showing the best thermal insulation performance among gases and generating only a difference of about 10% from the vacuum. Considering the possible maintenance issues of maintaining the vacuum inside the MCV throughout the operation period, this small difference can reduce the dependence on the vacuum concept. In other words, these results may suggest the feasibility of the MCV system using the gas gap filler.

## 4. Conclusion

An evaluation of the difference in the unnecessary heat loss caused by changes in the gap filler material under normal operating conditions of the ATOM was performed by using the ANSYS FLUENT code.

First, through the streamline analysis, it was confirmed that the natural convection flow in gas is faster than in vacuum condition. It was also confirmed that when radiation heat transfer is considered, the velocity of the flow is relatively slower.

If the radiation heat transfer is not considered, the calculated heat loss was significantly lower in the vacuum condition. However, if radiation heat transfer is considered, the flow rate in vacuum is still 1/3 times slower than for gas gap fillers, but the difference in heat loss is reduced to the level of 10-20%.

It is judged that the vacuum gap condition can be replaced effectively by a gas gap filler in the perspective of heat loss. However, there are many additional considerations to assert the substitutability of the gas gap filler through the calculation results. In particular, the comparison between the cost of maintaining the vacuum condition and the cost due to the increased heat loss is remains a future work.

#### **ACKNOWLEDGEMENT**

This research was supported by the National Research Foundation of Korea (NRF), funded by the Ministry of Science, ICT, and Future Planning, the Republic of Korea (No. NRF-2016R1A5A1013919) and the Nuclear Safety Research Program through the Korea Foundation of Nuclear Safety (KoFONS) using the financial resource granted by the Nuclear Safety and Security Commission (NSSC) of the Republic of Korea (grant number 2003006-0120-CG100).

#### **REFERENCES**

- [1]. H. Subki, "ADVANCES IN SMALL MODULAR REACTOR TECHNOLOGY DEVELOPMENTS", 11, IAEA, Vienna, and Austria (2020).
- [2]. M.D. Carelli et al., "Economic features of integral, modular, small-to-medium size reactors," *Progress in Nuclear Energy*, 52 (4), pp. 403-414 (2010).
- [3]. D.T. Ingresoll et al., "NuScale small modular reactor for Co-generation of electricity and water," *Desalination*, 340, pp. 84-93 (2014).
- [4]. C.A. Lloyd et al., "Transport, constructability, and economic advantages of SMR modularization," *Progress in Nuclear Energy*, 134, (2021).
- [5]. Y. Kim, "Conceptual Development of an Autonomous Small Modular Reactor," MIT-KAIST Symposium, March 30, 2017
- [6]. X.H. Nguyen et al., "An advanced core design for a soluble-boron-free small modular reactor ATOM with centrally-shielded burnable absorber," *Nuclear Engineering and Technology*, 51(2), pp. 369-376 (2019).
- [7]. M.W. Na et al., "Indefinite sustainability of passive residual heat removal system of small modular reactor using dry air cooling tower," *Nuclear Engineering and Technology*, Vol. 52, pp. 964-974 (2020).

[8] NuScale Power, "Status Report-NuScale SMR (NuScale Power, LLC)", NuScale Power, United States of America (2020).